Computer Assisted Mechanics and Engineering Sciences, **14**: 209–217, 2007.


# Dynamic soil profile determination with the use of a neural network

Janusz Kogut
*Institute of Structural Mechanics, Cracow University of Technology, Cracow, Poland*

(Received in the final form April 6, 2007)

This paper describes an application of feedforward neural network to analyse the SASW (Spectral Analysis of Surface Waves) measurements of the soil. The free field dynamic experiment was performed to determine the soil dynamic properties. An inversion process is based on the comparison of experimental and theoretical phase velocity curves. The results of the experiment are pre-processed by a neural network. The dynamic soil profile is compared with the real soil profile based on the geotechnical site prospect.

## 1. Introduction

The Spectral Analysis of Surface Waves (SASW) is a non-destructive, and a non-invasive geotechnical prospection method performed to determine horizontal layering of a soil, or e.g. a layered strip or plate. It may be applied to obtain near-surface site characteristics such as dynamic Young elastic moduli, layer thickness and/or Poisson ratio estimate for small strains. One of the objectives of this method is to estimate the experimental dispersion curve, describing the relationship between the propagation velocity of the Rayleigh waves and frequency. Furthermore, an inversion process based on the comparison of the results of experimental and theoretical phase velocity curves is needed. The procedure generally assumes horizontal, isotropic, elastic and homogeneous layers.

A number of authors described theoretical solutions for the SASW method, e.g. [5, 6]. Al-Hunaidi [1] applied the multiple filter and cross correlation technique to process SASW signals. Williams and Gucunski [13] used a neural network approach to the SASW tests for training the back-propagation (BPNN) and general regression neural networks (GRNN). Furthermore, the networks have been applied to the inversion procedure in which dynamic soil characteristics have been obtained with satisfactory results.

In the present paper artificial neural networks are applied to process SASW signals instead of the technique described in [1]. The free field dynamic experiment results are pre-processed and then used to obtain the alternative experimental phase velocity curve. Furthermore, the soil dynamic characteristics are determined, using Kausel dynamic stiffness matrix, alternatively to Pyl and Degrande [11]. The dynamic soil profile is compared with the results of intrusive methods used at the test site, such as SCPT (Seismic Cone Penetration Test) and borehole tests performed there [7].

## 2. Soil characteristics

### 2.1. The test site

The test site is located on a field between the Rue de la Bruyère and the High Speed Train track Brussels–Cologne in Lincent, Belgium. Figure 1 presents the site as well as all the characteristic points and distances. An elaborated soil testing campaign was performed by TucRail — Belgian track construction company in preparation of the construction works on the track. The tests included

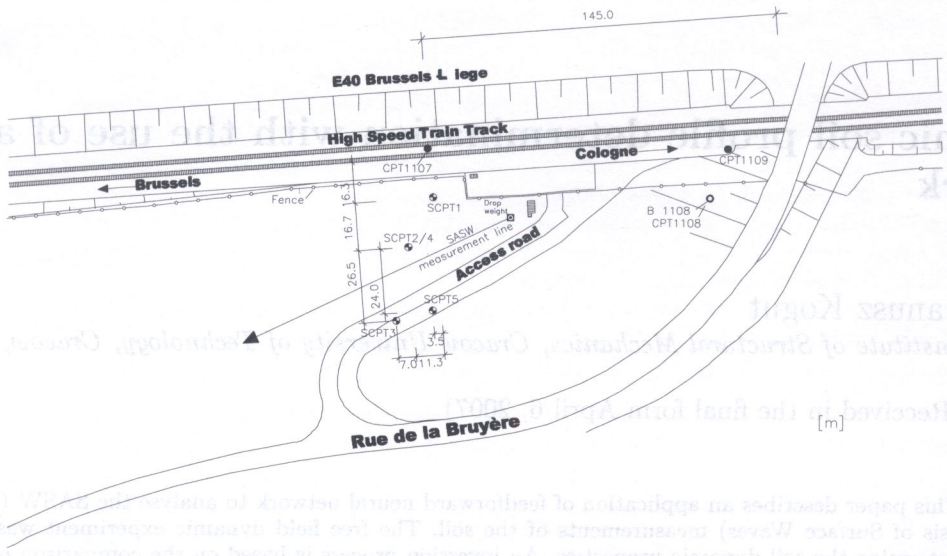


**Fig. 1.** Plan of the test site in Lincent, Belgium

boring, undisturbed sampling, soil classification, conventional cone penetration tests (CPT) and the ground water table monitoring.

### 2.2. Soil stratification

The soil in Lincent consists of a tertiary and quaternary deposits. The drilling B1108 (Fig. 1) is located closest to the test site. It reveals a shallow quaternary top layer of silt with the thickness of 1.20 m, followed by a 2.00 m thick layer of fine sand (Fig. 2), and a sequence of 4.30 m thick stiff layers of arenite embedded in clay. Below that a 1.00 m thick layer of clay followed by a 1.50 m thick layer of fine sand, and thin layers of fine sand and clay are found. The sediments located between 1.00 and 13.00 m belong to the tertiary formation of Hannut, while the subsequent layers refer to the tertiary formation of Heers. Deeper borings reveal the formation of porous chalk at the depth of about 30.00 m. The ground water table was monitored at the boring B1108. The ground water depth varied between 6.00 and 12.20 m with a mean value of 10.40 m. The CPT and, later on, SCPT tests were limited to the depth of 6.50 m due to the existence of stiff layer of arenites.

### 2.3. Seismic Cone Penetration Tests (SCPT)

Several complementary in situ dynamic tests were performed to determine the soil stratification and the dynamic properties of the soil, including five SCPT tests [7]. The SCPT is an intrusive geotechnical prospection method allowing to estimate the body wave velocities and the material damping ratios of the soil at depth with a resolution dependent on the distance of the receivers mounted in the cone (usually between 0.50 and 1.00 m). The results of such tests are highly complementary with the SASW tests performed on site. Figure 3 displays a shear wave velocity profile derived from the SCPT tests mentioned above. Preliminary SCPT tests 1–3 were performed during the winter and with the cone containing geophones. The last two SCPT tests were performed during the summer with the accelerometers located inside a new cone. The differences in the results cannot be readily explained. Hence they are split and the new cone results are used later on in comparisons.

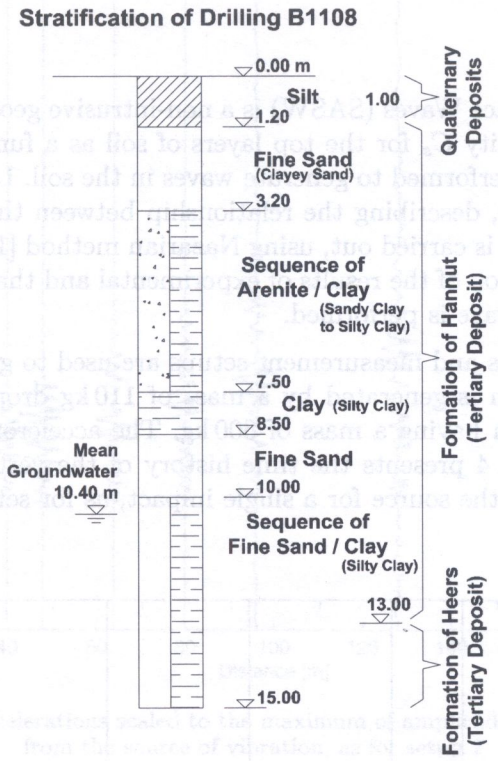


**Fig. 2.** Soil stratification and lithological description of the profile at Lincent site

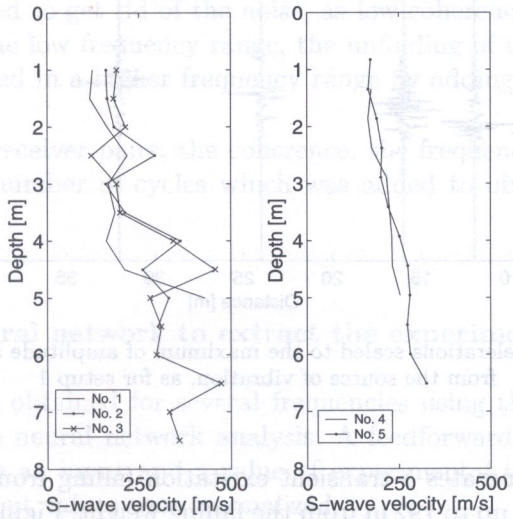


**Fig. 3.** Shear wave velocity profile derived from SCPT tests results

## 3. Spectral analysis of surface waves

### 3.1. Experimental results

The Spectral Analysis of Surface Waves (SASW) is a non-intrusive geotechnical prospection method used to determine shear velocity $C_s$ for the top layers of soil as a function of depth. At first, field tests with a falling mass are performed to generate waves in the soil. Later on, the estimation of the experimental dispersion curve, describing the relationship between the propagation velocity of the Rayleigh waves and frequency is carried out, using Nazarian method [10]. Furthermore, an inversion process based on the comparison of the results of experimental and theoretical phase velocity curves for the fundamental surface wave is performed.

Two different falling devices and measurement setups are used to generate surface waves [11]. In setup 1, a transient excitation is generated by a mass of 110 kg dropped from a height of 0.90 m onto a square steel foundation having a mass of 600 kg. The accelerometers are placed up to 48 m from the falling mass. Figure 4 presents the time history of the vertical free field acceleration as function of the distance from the source for a single impact, as for setup 1.

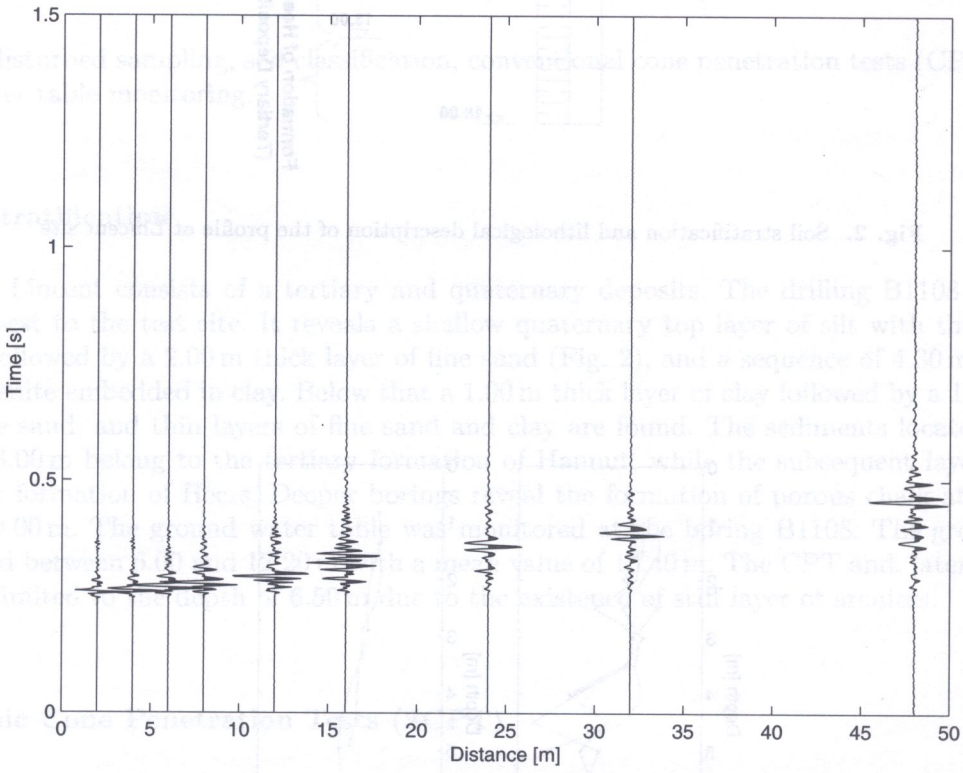


**Fig. 4.** Vertical free field accelerations scaled to the maximum of amplitude as a function of the distance from the source of vibration, as for setup 1

In setup 2, 600 kg mass generates a transient excitation falling from 0.85 m on a circular plate. The accelerometers are placed up to 192 m from the falling weight. Figure 5 presents the time history of the vertical free field acceleration as function of the distance from the source for a single impact, as for setup 2. In both Figs. 4 and 5 accelerations have been scaled so that the attenuation with an increasing distance to the source, due to the geometrical and material damping in the soil, can be better appreciated.

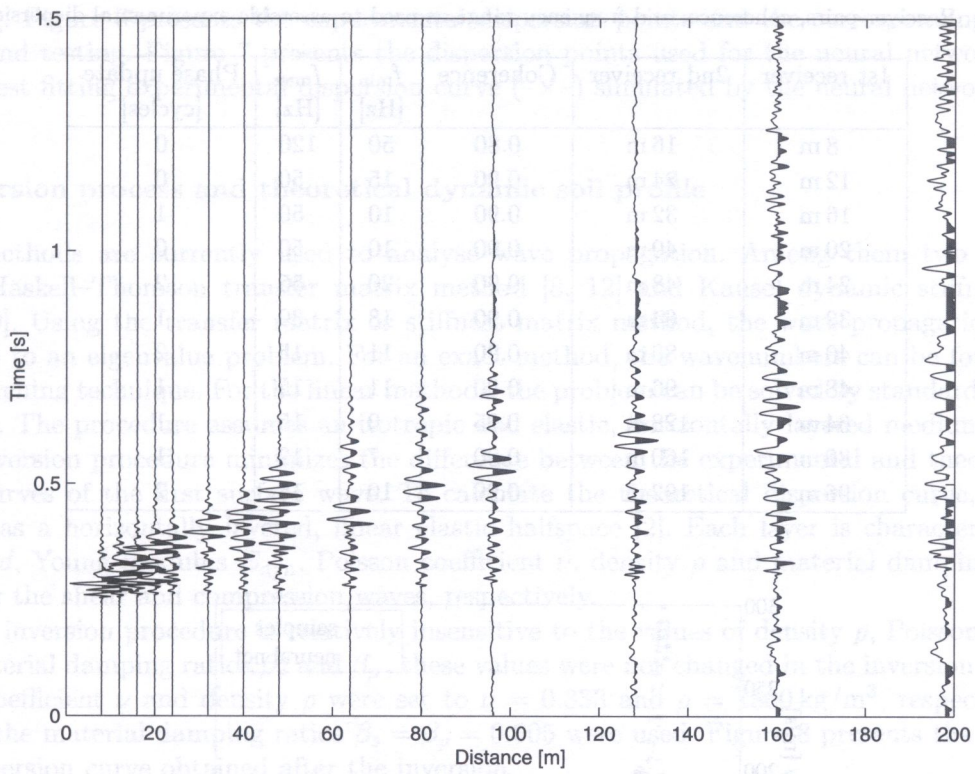


**Fig. 5.** Vertical free field accelerations scaled to the maximum of amplitude as a function of the distance from the source of vibration, as for setup 2

### 3.2. Assembling of the experimental dispersion curve

Ten events from setup 2 are used to determine the shear wave velocity $C_s$ for the top layers as a function of depth $z$. The phase velocity $C_R$ of the first surface wave mode is determined as a function of frequency $f$, using Nazarian method [3]. This method is based on cross power spectra and coherence function of the response spectra for receiver pairs in the free field. A threshold for the coherence function is used to get rid of the noise, as low coherence indicates poor data quality. Due to a low coherence in the low frequency range, the unfolding of the phase might be erroneous; the phase is therefore updated in a higher frequency range by adding a number of cycles to obtain the actual phase.

Table 1 summarizes the receiver pairs, the coherence, the frequency range where the quality of data is good and the final number of cycles which was added to obtain the actual phase in this frequency range.

### 3.3. Application of a neural network to extract the experimental dispersion curve

535 dispersion samples were obtained for several frequencies using the Nazarian method. The file was used as an input to the neural network analysis. A feedforward neural network was applied. Frequency value was used as an input and a value of experimental phase velocity was used as an output. Both input and output values were normalized.

Two hidden layers of 32 neurons each were applied. The neural network structure was 1-32-32-1. The initial neuron weights were set up randomly from the range of $[-0.3, 0.3]$. The resilient back-propagation algorithm was used for neural training. The network was trained and tested several times, each time using randomly selected 70–80% of samples for training, and 20–30% of samples

**Table 1.** Receiver pairs, coherence, and frequency range as used to assemble experimental dispersion curve

| 1st receiver | 2nd receiver | Coherence | $f_{min}$ [Hz] | $f_{max}$ [Hz] | Phase update [cycles] |
|---|---|---|---|---|---|
| 8 m | 16 m | 0.80 | 50 | 120 | 0 |
| 12 m | 24 m | 0.90 | 15 | 50 | 0 |
| 16 m | 32 m | 0.90 | 10 | 50 | 1 |
| 20 m | 40 m | 0.90 | 10 | 50 | 0 |
| 24 m | 48 m | 0.90 | 20 | 55 | 2 |
| 32 m | 64 m | 0.90 | 18 | 30 | 1 |
| 40 m | 80 m | 0.90 | 11 | 15 | 2 |
| 48 m | 96 m | 0.90 | 11 | 15 | 1 |
| 64 m | 128 m | 0.95 | 0 | 15 | 1 |
| 80 m | 160 m | 0.90 | 7 | 12 | 1 |
| 96 m | 192 m | 0.90 | 10 | 15 | 2 |

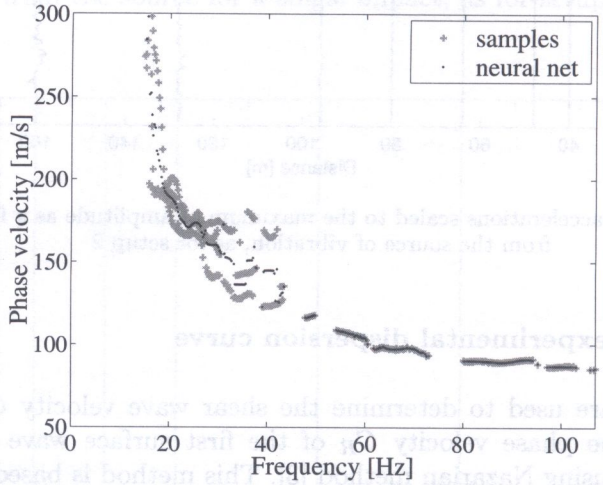


**Fig. 6.** Experimental dispersion points (+), and corresponding results from the neural network (dots)

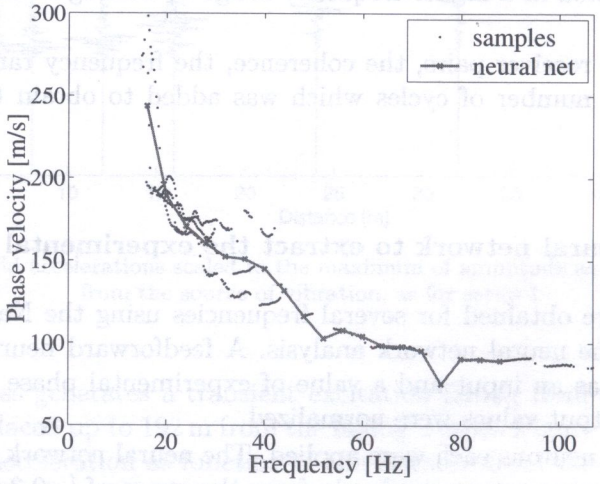


**Fig. 7.** Dispersion points used for the neural network analysis (dots). Superimposed on that is the experimental (–×–) dispersion curve simulated by the neural network

for testing. Figure 6 presents the experimental dispersion points and the corresponding results of training and testing. Figure 7 presents the dispersion points used for the neural network analysis and the best fitting experimental dispersion curve (–×–) simulated by the neural network.

### 3.4. Inversion process and theoretical dynamic soil profile

Several methods are currently used to analyse wave propagation. Among them two are widely applied: Haskell–Thomson transfer matrix method [8, 12] and Kausel dynamic stiffness matrix method [9]. Using the transfer matrix or stiffness matrix method, the wave propagation problem is reduced to an eigenvalue problem. For an exact method, the wavenumbers can be found e.g. by a root searching technique. For the linear methods, the problem can be solved by standard eigenvalue solvers [4]. The procedure assumes an isotropic and elastic, horizontally layered medium.

The inversion procedure minimizes the difference between the experimental and theoretical dispersion curves of the first surface wave. To calculate the theoretical dispersion curve, the soil is modelled as a horizontally layered, linear elastic halfspace [2]. Each layer is characterized by its thickness $d$, Young modulus $E_{\mathrm{dyn}}$, Poisson coefficient $\nu$, density $\rho$ and material damping ratios $\beta_s$ and $\beta_p$ for the shear and compression waves, respectively.

As the inversion procedure is relatively insensitive to the values of density $\rho$, Poisson coefficient $\nu$ and material damping ratios $\beta_s$ and $\beta_p$, these values were not changed in the inversion procedure. Poisson coefficient $\nu$ and density $\rho$ were set to $\nu = 0.333$ and $\rho = 1800\,\mathrm{kg/m^3}$, respectively. Low values of the material damping ratios $\beta_s = \beta_p = 0.005$ were used. Figure 8 presents the theoretical (–o–) dispersion curve obtained after the inversion.

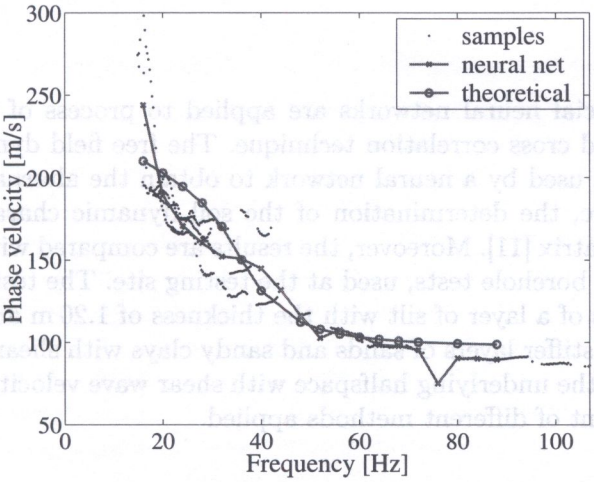


**Fig. 8.** The experimental (–×–) dispersion curve simulated by the neural network and the theoretical (–o–) dispersion curve obtained after inversion process superimposed on the discrete points from the experiment (dots)

The initial profile parameters in every inversion step were estimated using the final profile for the case of one, two and three layers on a halfspace. Table 2 shows thickness $d$ and shear wave velocity $C_s$ of the final profile for the case of four layers on a halfspace. The results show a soft layer with a shear wave velocity of about 105 m/s and three layers with a shear wave velocities of between 213 m/s and 239 m/s on top of the stiffer halfspace.

The results of the SASW demonstrate that the site consists of a layer having the thickness of 1.20 m and a shear wave velocity of 105 m/s over several stiffer layers with the shear wave velocities between 213 m/s and 239 m/s upon the underlying halfspace with a shear wave velocity of 252 m/s. Figure 9 shows the shear wave velocity profile of the Lincent site derived from SASW results.

**Table 2.** Soil dynamic parameters

| Layer | $d$ [m] | $E_{dyn}$ [$10^6$ N/m$^2$] | $C_p$ [m/s] | $C_s$ [m/s] | $\nu$ [–] | $\rho$ [kg/m$^3$] |
|---|---|---|---|---|---|---|
| 1 | 1.16 | 53 | 210 | 105 | 0.333 | 1800 |
| 2 | 0.79 | 247 | 454 | 227 | 0.333 | 1800 |
| 3 | 0.52 | 218 | 426 | 213 | 0.333 | 1800 |
| 4 | 0.12 | 274 | 478 | 239 | 0.333 | 1800 |
| 5 | $+\infty$ | 305 | 505 | 252 | 0.333 | 1800 |

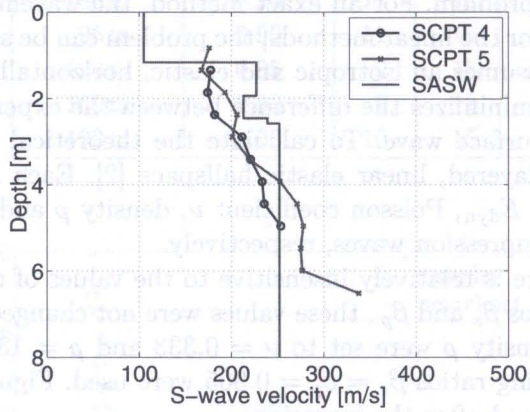


**Fig. 9.** Comparison of the shear wave velocity profiles derived from SCPT and SASW results

## 4. Conclusions

In the present paper artificial neural networks are applied to process of SASW signal instead of using the multiple filter and cross correlation technique. The free field dynamic experiment results are pre-processed and then used by a neural network to obtain the alternative experimental phase velocity curve. Furthermore, the determination of the soil dynamic characteristics is done, using Kausel dynamic stiffness matrix [11]. Moreover, the results are compared with the results of intrusive methods – SCPT tests and borehole tests, used at the testing site. The tests performed on the spot reveal that the site consists of a layer of silt with the thickness of 1.20 m and shear wave velocity of about 105 m/s over several stiffer layers of sands and sandy clays with shear wave velocities between 213 m/s and 239 m/s upon the underlying halfspace with shear wave velocity of 252 m/s. The results demonstrate good agreement of different methods applied.

## Acknowledgments

The results presented in this paper have been obtained within the frame of project 4 T07E 055 27 *Traffic induced vibrations – numerical modelling with experimental validation.* The financial support of the Polish State Committee for Scientific Research is kindly acknowledged.

## References

[1] M.O. Al-Hunaidi. Analysis of dispersed multi-mode signals of the SASW method using the multiple filter/crosscorrelation technique. *Soil Dynamics and Earthquake Engineering*, **13**: 13–24, 1994.

[2] G. Degrande, W. Alaerts. *Spectral Version 7.01: A Direct Stiffness Formulation for Harmonic and Transient Wave Propagation in Layered Dry, Saturated and Unsaturated Poroelastic Media.* User's manual, Department of Civil Engineering, Katholieke Universiteit Leuven, 1999.

[3] W. Dewulf, G. Degrande, G. De Roeck. *Practical Application of the SASW Method.* Internal report 37-BWM-03, Department of Civil Engineering, Katholieke Universiteit Leuven, June 1995. IWONL research grant CI 1/4-7672/091.

[4] V. Ganji, N. Gucunski, S. Nazarian. Automated inversion procedure for spectral analysis of surface waves. *Journal of Geotechnical and Geoenvironmental Engineering, Proceedings of the ASCE*, **124**(8): 757–770, 1998.

[5] N. Gucunski, R.D. Woods. Use of Rayleigh modes in interpretation of SASW test. In *Proceedings of the 2nd International Conference on Recent Advances in Geotechnical Earthquake Engineering and Soil Dynamics*, Vol. **II**: 1399–1408, University of Missouri, St. Louis, 1991.

[6] N. Gucunski, R.D. Woods. Numerical simulation of the SASW test. *Soil Dynamics and Earthquake Engineering*, **11**: 213–227, 1992.

[7] W. Haegeman. *In Situ Tests Retie–Waremme–Lincent.* Report RUG IV.1.16.3, Soil Mechanics Laboratory, Ghent University, September 2001. STWW Programme Technology and Economy, Project IWT-000152.

[8] N.A. Haskell. The dispersion of surface waves on multilayered media. *Bulletin of the Seismological Society of America*, **73**: 17–43, 1953.

[9] E. Kausel, J.M. Roësset. Stiffness matrices for layered soils. *Bulletin of the Seismological Society of America*, **71**(6): 1743–1761, 1981.

[10] S. Nazarian, M.R. Desai. Automated surface wave method: field testing. *Journal of Geotechnical Engineering, Proceedings of the ASCE*, **119**(7): 1094–1111, 1993.

[11] L. Pyl, G. Degrande. *Determination of the Dynamic Soil Characteristics with the SASW Method at a Site in Lincent.* Report BWM-2001-02, Department of Civil Engineering, Katholieke Universiteit Leuven, August 2001. STWW Programme Technology and Economy, Project IWT-000152.

[12] W.T. Thomson. Transmission of elastic waves through a stratified solid medium. *Journal of Applied Physics*, **21**: 89–93, 1950.

[13] T.P. Williams, N. Gucunski. Neural networks for backcalculation of moduli from SASW test. *Journal of Computing in Civil Engineering, Proceedings of the ASCE*, **9**(1): 1–8, 1995.